811313

Application of Modal Modeling and Mount System Optimization to Light Duty Truck Ride Analysis

Alan E. Duncan
Chevrolet Motor Div.
General Motors Corp.

ABSTRACT

A basic review of vehicle modal modeling techniques is presented and applied to determine the vibrational shake characteristics of a light duty pickup truck subjected to tire force variation and random road surface dynamic loads. Comparisons of natural vibration frequencies and random road response between a prototype pickup and the vehicle model are presented to establish the level of correlation.

A computer optimization technique is applied to tune the body, engine, and transmission mount system of the vehicle model until the vibration levels are minimized. Simultaneous reduction in road and tire induced vibration response of the model is achieved.

THE REQUIREMENT TO PRODUCE fuel efficient vehicles at productivity levels that will be cost competitive in the world market is the most recent challenge to face the domestic automotive market. Standards for occupant protection, exhaust emissions, bumper damagability, and other government regulations, as well as increasing material costs, emphasize the need for vehicles with optimum mass efficiency and structural integrity.

The finite element analysis method has provided the structural analyst with a tool to predict the structural performance of a vehicle well in advance of fabrication of prototype parts. The value of the approach results from the ability to enhance the effectiveness of management decision making among design alternatives that are in the initial concept phase. With timely and accurate analysis support, management can assure that the final compromise between structure, packaging, styling, regulation, and manufacturing will provide a vehicle nearer the optimum of customer satisfaction.

The vehicle system model is one finite element approach for studying the vibration behavior of the structure. The purpose of this paper is to provide a background for the vehicle system model approach and to apply a method to improve the ride quality of a light duty pickup truck using an optimization technique. The optimization algorithm systematically varies the properties of the body and engine mounting rubber isolators until the vibration levels are minimized.

The following topics are discussed:

1. Theory behind modal modeling using the finite element approach with some details of the truck vehicle model.
2. A discussion of the dynamic load sources used to analyze the vibration response.
3. A comparison between a prototype vehicle measurement and the vehicle model prediction of natural vibration frequency and random road response, to establish the level of correlation.
4. A discussion of the optimization technique and procedure.
5. A comparison of vibration response between the original and optimized mounting system of the vehicle model.

MODAL SYNTHESIS THEORY AND MODELING

The terms modal synthesis are used to describe a process by which the dynamic model of a vehicle system is synthesized from the dynamic or modal characteristics of its major sybsystems called modal components (1).* The major modal components of the light duty truck studied here were: the front end sheet metal (FESM), cab, pickup box, and frame. These modal components are assembled together, along with suspension and driveline, to result in a modal representation of the complete vehicle for the study of vibration characteristics in the ride frequency range from 5 to 25 hz. Butkunas (2) remarks that the ride frequency range, from .5 to 25 hz is characterized by "vibration sensation" that is "felt" by the passenger; whereas, "at higher frequencies the perception of vibrational motion diminishes and gradually the perception of vibration as noise takes over." This paper will consider the ride range from 5 to 25 hz since response below 5 hz is unaffected by the changes in mounting system that will be presented.

* Numbers in parenthesis indicate references at the end of the paper.

0096-736X/82/9004-4075$02.50

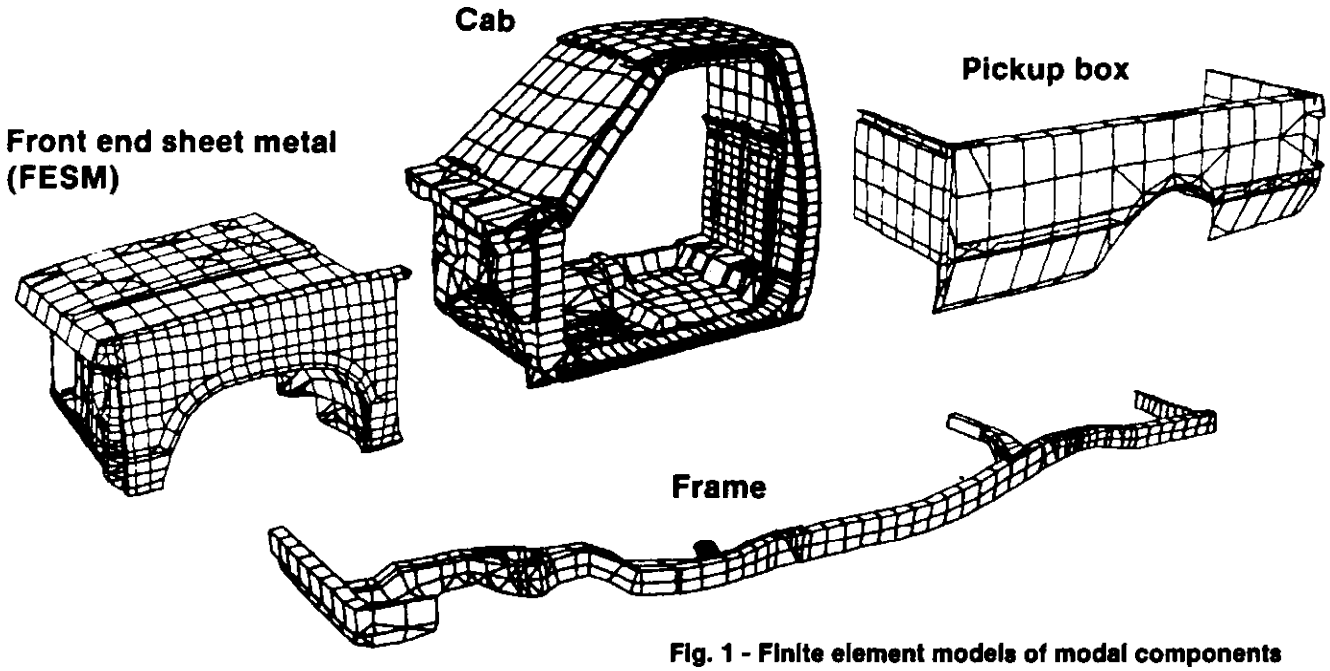

Fig. 1 - Finite element models of modal components

Prior to obtaining the modal properties for the system, each component is modeled as in Fig. 1 and analyzed as a separate structure. One-half of each component was modeled since they were nearly symmetric relative to the vehicle centerline and were analyzed by applying the appropriate boundary condition along the centerline. In general, the fine mesh modeling detail is not needed to find the component modal properties. A simpler plate model with bar elements to represent main structural sections would have been sufficient if the joint efficiencies at the section junctions were known (3). Since joint efficiencies were not known, the truck structure was modeled in detail; however, this detail was also required for a static stiffness and stress analysis.

A static analysis of the components is performed for beaming and torsional stiffness and for the presence of high stress areas in the overall structure. A dynamic analysis is used to study the component's natural vibration modeshapes. The analysis is compared with past tests or analysis and, along with engineering experience, is used to decide if a design change for the component is warranted. In addition to providing early design direction and insight into the behavior of the individual components, these steps provide a check on the component subsystem to assure that potential modeling errors are corrected.

Once the final design configuration is modeled and checked, the normal modes for the component are determined from the equation of motion for free vibration (4, 5).

$$[m]\{\ddot{x}\} + [k]\{x\} = 0 \qquad (1)$$

where

m = structural mass matrix
k = structural stiffness matrix
x = physical displacement degree of freedom

Assuming harmonic motion (6) substitute

$$\{x\} = \{x_o\}\, e^{j\omega t}$$

where

$\{x_o\}$ = the amplitude of vibration
$e^{j\omega t}$ = the harmonic time function

$j = \sqrt{-1}$

$\omega = 2\pi f$ where f = frequency in hz

to get the following

$$\{-\omega^2[m] + [k]\}\{x_o\} = 0 \qquad (2)$$

This is the form of the eigenvalue problem (4) which can be solved by most general purpose structural analysis programs, in this case NASTRAN, for the natural frequencies ω_i and modeshapes $\{\phi_i\} = \{x_o\}_i$. If there are n degrees of freedom (DOFs) in the dynamic analysis, then there will be n each of natural frequencies and modeshapes. It should be noted that the eigenvalue solution for each component requires, for economy, a Guyan (7) reduction from the full set of DOFs used for static analysis to a dynamic analysis set that is approximately 5 to 10% of the static DOFs. The nature of the Guyan approximations has been discussed by Nelson

(8). For simplicity, the discussion here assumes that the static and dynamic DOFs are identical.

Using the modeshapes, a transformation can be made from physical to modal DOFs (9) with the following:

$$\{x_o\} = [\phi]\{s\} \tag{3}$$

where

$[\phi]$ is the matrix of modeshapes.

$\{s\}$ is the vector of scale factors for the modeshapes called modal coordinates or modal DOFs.

Expanding equation 3 gives the following:

$$\begin{Bmatrix} x_{o1} \\ x_{o2} \\ \vdots \\ x_{on} \end{Bmatrix} = \begin{Bmatrix} \vdots \\ \phi_1 \\ \vdots \end{Bmatrix} s_1 + \begin{Bmatrix} \vdots \\ \phi_2 \\ \vdots \end{Bmatrix} s_2 + \cdots \begin{Bmatrix} \vdots \\ \phi_n \\ \vdots \end{Bmatrix} s_n = [\phi]\{s\} \tag{4}$$

Thus it can be seen that the unknown displacement can be expressed as a sum of known modeshapes each scaled by the unknown modal coordinate. Next, substitute the transformation into Eq. 2 and pre-multiply by $[\phi]^T$ to get:

$$\{-\omega^2[\phi]^T[m][\phi]+[\phi]^T[k][\phi]\}\{s\} = 0 \tag{5}$$

An important property of $[\phi]$ is that it will diagonalize [m] and [k] (4) resulting in:

$[\phi]^T[k][\phi] = \lceil K \rfloor$ the diagonal modal stiffness matrix and

$[\phi]^T[m][\phi] = \lceil M \rfloor$ the diagonal modal mass matrix Eq. 5 becomes

$$\{-\omega^2\lceil M\rfloor+\lceil K\rfloor\}\{s\} = 0 \tag{6}$$

Therefore, once $[\phi]$ is obtained from the eigenvalue analysis, it can be used to transform from the physical mass and stiffness matrix relationship to the more compact diagonalized modal mass and stiffness relationship.

Writing the equation for any of the i-th rows of Eq. 6 gives

$$\{-\omega^2 M_i + K_i\} s_i = 0$$

solving for ω gives

$$\omega_i = \sqrt{K_i / M_i}$$

but this is exactly equal to the i-th natural frequency of the system. K_i and M_i, termed the modal stiffness and modal mass, respectively, are related to the natural frequency of mode i by the same relationship as that of a one degree of freedom spring-mass system.

The transformation relationship from physical to modal DOFs $\{x_o\} = [\phi]\{s\}$ replaces $\{x_o\}$ as an unknown in the equations by $\{s\}$ which is a vector of scale factors which multiply by each of the modeshapes as shown in Eq. 4. Stated another way, this says that any deformation state of the structure $\{x_o\}$ can be specified as a linear combination of all its modeshapes $[\phi]\{s\}$.

This modal transformation is exact if all of the modes are retained for the modal representation to be used in the vehicle model. However, this would be cost prohibitive and is unnecessary since only the dynamic characteristics below 25 hz are of interest for this model. Therefore, the component is represented in the vehicle model by a reduced set of modeshapes consisting of its lowest vibration modeshapes and corresponding modal masses and stiffnesses.

Benfield (1) has shown that the lowest free vibration modes of the complete system can be found from the free vibration modes of the components, if a sufficient number of modes are retained to represent the component in the system. If only m modes are retained to describe the component, then the modal transformation is

$$\underset{n\times 1}{\{x_o\}} = \underset{n\times m}{[\phi_1\ \phi_2 \cdots \phi_m]}\ \underset{m\times 1}{\{s_m\}}$$

The modes from m + 1 to n have been truncated and are not used in the vehicle analysis. The physical interpretation of this truncation means that, of the original n DOFs to describe the deformation state of the component $\{x_o\}$, only m DOFs are remaining to describe the component's deformation in the vehicle model. Clearly, the m modes retained for each component must have sufficient modal definition to provide an accurate vehicle dynamic representation in the ride frequency range below 25 hz. For the truck vehicle model, the modes retained for each component were the following:

1. Front end sheet metal (FESM) = 60 modes

2. Cab = 40 modes

3. Pickup box = 40 modes

4. Frame = 30 modes

The equation of motion for the component becomes

$$\{-\omega^2\lceil M_m\rfloor + \lceil K_m\rfloor\}\{s_m\} = 0$$

and is now an m DOF system of equations. Since each component is represented in the vehicle system by its lowest modes, it is referred to as a modal model or modal body.

A post processor to NASTRAN developed by General Motors Engineering Staff, called GETMODE, extracts the modal body representation from the results of a

NASTRAN eigenvalue analysis. Modal viscous damping for each mode can also be included as a percentage of critical damping. The amount of modal damping for a component is based on typical values obtained from past modal testing.

The component equation of motion for forced vibration with damping included then becomes

$$\{-\omega^2 [M] + j\omega [C] + [K]\} \{s_m\} = [\phi]^T \{f\} = \{F_s\} \quad (7)$$

where

[C] is the modal viscous damping matrix

{f} is the physical DOF force vector

$\{F_s\}$ is called the modal force vector

The next step towards the complete vehicle model is to assemble the modal bodies. A residual compliance must be added to each modal body at the connection points between components that are rigidly bolted together. The residual compliance, also called local compliance (10), accounts for the compliance of the component that is neglected when the higher modes are truncated. McClelland (9) presents a detailed derivation of residual compliance and the exact form to account for modal truncation error. The residual compliance from both componets can be reduced to a single equivalent compliance at the connection. Residual compliance for the truck model was included at the FESM-cab interface. Only the FESM compliance was calculated at the connections, since the cab was assumed to be much less compliant. Thus, the FESM compliance represented the equivalent spring rate at the connection between the two structures.

A residual compliance is usually not necessary when two components are connected with a rubber isolator mount. The mount is generally much more compliant than the residual compliance so that the equivalent rate of the connection is close to that of the mount alone. Davis (10) shows that the residual compliance has a significant effect on the results when it approaches the same rate as the mount.

The connection between components, whether residual compliance or rubber mount, is modeled using a simple one dimensional spring element as shown in Fig.

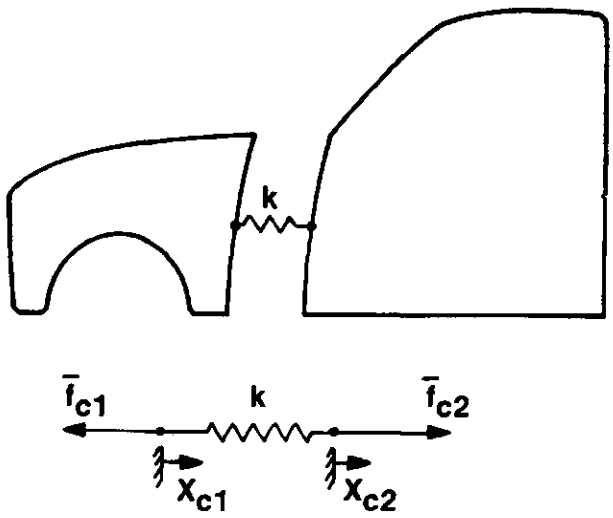

Fig. 2 - Inter-component spring connection

2. The connection locations on each component are separated for illustration but in actuality would be coincident. The spring rate, k, is the equivalent rate, accounting for the residual compliance of both components.

The relationship between the spring connection element and the modal body representations will now be considered. For each component in Fig. 2, the free vibration equation is:

Component 1

$$\{-\omega^2 [M_1] + [K_1]\} \{s_1\} = 0$$

and

$$\{x_1\} = [\phi_1] \{s_1\}$$

Component 2

$$\{-\omega^2 [M_2] + [K_2]\} \{s_2\} = 0$$

and

$$\{x_2\} = [\phi_2] \{s_2\}$$

The attachment spring between the two components in Fig. 2 has the following equation:

$$\begin{bmatrix} k & -k \\ -k & k \end{bmatrix} \begin{Bmatrix} x_{c1} \\ x_{c2} \end{Bmatrix} = \begin{Bmatrix} \bar{f}_{c1} \\ \bar{f}_{c2} \end{Bmatrix}$$

Partition x and f for each component as follows:

$$\{x\} = \begin{Bmatrix} x_r \\ \dots \\ x_c \end{Bmatrix} \text{ and } \{f_c\} = \begin{Bmatrix} \bar{f}_r \\ \dots \\ \bar{f}_c \end{Bmatrix} = \begin{Bmatrix} 0 \\ \dots \\ \bar{f}_c \end{Bmatrix}$$

$\{x_c\}$ is the component displacement at the connection point.

$\{x_r\}$ are the remaining component displacement DOFs.

$\{\bar{f}_c\}$ is the force in the spring at the connection.

let $$[K_c] = \begin{bmatrix} 0 & \cdots & 0 \\ \vdots & \ddots & \vdots \\ 0 & \cdots & k \end{bmatrix}$$

then $$\begin{bmatrix} K_c & -K_c \\ -K_c & K_c \end{bmatrix} \begin{Bmatrix} x_1 \\ x_2 \end{Bmatrix} = \begin{Bmatrix} f_{c1} \\ f_{c2} \end{Bmatrix}$$

Noting that the force on the modal body is equal and opposite to the spring force, the complete set of equations for both components and spring can be written:

$$\left\{ -\omega^2 \begin{bmatrix} [M_1] & & \\ & [M_2] & \\ & & 0 \end{bmatrix} + \begin{bmatrix} [K_1] & & & \\ & [K_2] & & \\ & & \begin{bmatrix} K_c & -K_c \\ -K_c & K_c \end{bmatrix} \end{bmatrix} \right\} \begin{Bmatrix} s_1 \\ s_2 \\ x_1 \\ x_2 \end{Bmatrix} = \begin{Bmatrix} -\phi_1^T f_{c1} \\ -\phi_2^T f_{c2} \\ f_{c1} \\ f_{c2} \end{Bmatrix}$$

But x_1 and x_2 can be eliminated by introducing the modal relationship

$$\{x\} = [\phi]\{s\}$$

The transformation is written:

$$\begin{Bmatrix} s_1 \\ s_2 \\ x_1 \\ x_2 \end{Bmatrix} = \begin{bmatrix} 1 & 0 \\ 0 & 1 \\ \phi_1 & 0 \\ 0 & \phi_2 \end{bmatrix} \begin{Bmatrix} s_1 \\ s_2 \end{Bmatrix}$$

Substitute and pre-multiply by the transpose of the transformation to get:

$$\left\{ -\omega^2 \begin{bmatrix} [M_1] & \\ & [M_2] \end{bmatrix} + \begin{bmatrix} [K_1 + \phi_1^T K_c \phi_1] & -\phi_1^T K_c \phi_2 \\ -\phi_2^T K_c \phi_1 & [K_2 + \phi_2^T K_c \phi_2] \end{bmatrix} \right\} \begin{Bmatrix} s_1 \\ s_2 \end{Bmatrix} = \begin{Bmatrix} 0 \\ 0 \end{Bmatrix} \quad (8)$$

The right side goes to zero since the forces in the spring are internal and equal and opposite. Thus, the connection springs result in off diagonal terms in the modal stiffness matrix which couple the modal body representations together.

It should be noted that the coupling is performed by NASTRAN during the solution process and is transparent to the user. The user need only define a spring element between connection points of the modal bodies.

The equation of free vibration for all four components used to represent the truck vehicle can be shown to be:

$$\left\{ -\omega^2 \begin{bmatrix} [M_1] & & & \\ & [M_2] & & \\ & & [M_3] & \\ & & & [M_4] \end{bmatrix} + \begin{bmatrix} [K_1] & & & \\ & [K_2] & & \\ & & [K_3] & \\ & & & [K_4] \end{bmatrix} + \bar{\phi}^T \bar{K}_c \bar{\phi} \right\} \begin{Bmatrix} s_1 \\ s_2 \\ s_3 \\ s_4 \end{Bmatrix} = \{0\} \quad (9)$$

and

$$\{x_1\} = [\phi_1]\{s_1\}$$

$$\{x_2\} = [\phi_2]\{s_2\}$$

$$\{x_3\} = [\phi_3]\{s_3\}$$

$$\{x_4\} = [\phi_4]\{s_4\}$$

where $\bar{\phi}^T \bar{K}_c \bar{\phi}$ represents all the inter-component coupling terms.

It should be re-emphasized at this point that a component physical vector $\{x_i\}$ is not an independent DOF in the system but is constrained to be a linear combination of its modeshapes $[\phi]_i$. The independent variables are the modal coordinates $\{s_i\}$ which specify the content of each component's modes required to form the vehicle response.

Lastly, the suspension and driveline are added to the modal components to synthesize the complete vehicle representation. For the truck model, rubber isolator characteristics were obtained from physical testing and consisted of: (1.) Body mounts, (2.) Engine and transmission mounts, (3.) Suspension control arm and spring attachment bushings. The suspension and driveline components do not resonate in the vehicle ride region (5-25 hz) and, were modeled as completely rigid links with appropriate rigid body inertial properties from calculation or test. The rigid suspension and driveline components for the truck model were: (1.) Control arms, (2.) Spindle-hub-wheel combination, (3.) Engine-transmission combination, (4.) Steering linkage, (5.) Propshafts, and (6.) Rear axle.

The final form of the equation for the complete vehicle system model for forced vibration and including viscous and structural damping (9) can be shown to be

$$\{-\omega^2 [M] + j\omega [C] + j [Kg] + [K]\} \begin{Bmatrix} s \\ x_{sd} \end{Bmatrix} = \begin{Bmatrix} F_s \\ f_{sd} \end{Bmatrix} \quad (10)$$

where M, C, Kg and K are the vehicle mass, viscous damping, structural damping, and stiffness matrices which contain all of the modal body relations and coupling terms.

$\{x_{sd}\}$ are the physical DOFs for suspension and driveline

$\{F_s\}$ are modal forces

$\{f_{sd}\}$ are the physical applied forces on suspension and driveline

The forced vibration equation is solved by NASTRAN using a modal method. For this method, the free undamped modeshapes and natural frequencies of the complete vehicle are found first, and then a reduced set of these modes are used to diagonalize the mass and stiffness matrix for the complete vehicle as was done for each component. The damping matrices are also multiplied by the modeshape transformation which results in generally a sparse but non-diagonal matrix. The forced vibration solution is performed for the vehicle model using the reduced set of equations.

The advantages of using the modal method are:

1. The natural frequencies and modeshapes of the model provide physical insight to the problem vibrations.
2. The reduced set of equations and sparse matrices simplifies the dynamic equation solution.

DYNAMIC LOAD SOURCE DESCRIPTION

This section will discuss the nature of the dynamic loads experienced by the vehicle. The sources of vibration in the vehicle include wheel and tire unbalance, tire nonuniformity, engine unbalance and torque variation, rotating shaft unbalance, driveline resonance, and road surface irregularity. For the truck vibration optimization analysis, the two types of vibration inputs studied were:

1. Wheel unbalance and tire force variations
2. Random road surface input.

The vibration analyses performed assume that the system is linear which means that the input force is linearly related to the output response. This assumption implies that suspension travel must be small relative to suspension geometry and that spring elements of the model operate in the linear elastic region.

For a linear system (6), it can be shown that output displacement is related to input force by

$$x_o(\omega) = H(\omega) f_i$$

where $H(\omega)$ is the transfer function of the system and comes from the solution of eq. 10.

x_o is the harmonic output amplitude at the response point

f_i is the harmonic input amplitude at the forcing point

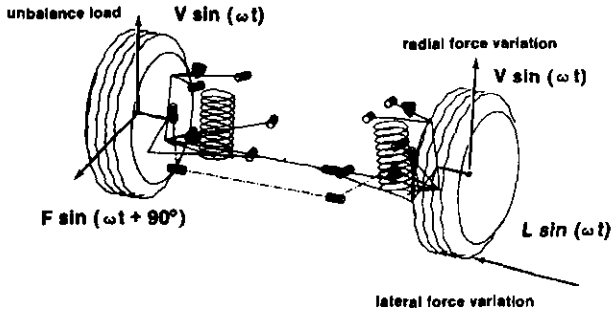

Fig. 3 - Tire-wheel dynamic load inputs

Wheel and tire inputs, as shown in Fig. 3, are strictly harmonic forcing functions which specify the amplitude f_i. There are several harmonics of the force associated with these inputs, but for this analysis the primary, or first, harmonic was chosen for study. Thus the response to a tire force input such as lateral force variation, as shown in Fig. 3, would be expressed as:

$$x_o(\omega) = H(\omega) \cdot L$$

Wheel unbalance, radial tire force, and lateral tire force variations were studied for each wheel separately resulting in twelve different harmonic response analyses.

The random road analysis is a study of the vehicle traversing typical road surfaces that might be experienced during actual service. The random road study is more complex due to the random nature of the road surface. The random road analysis of the truck vibration assumes that the vehicle is traversing a surface with unique right and left road profiles at a velocity of 72 Km/hr as shown in Fig. 4.

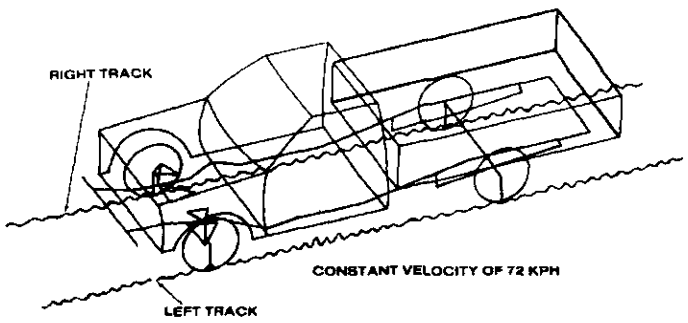

Fig. 4 - Random road surface input schematic

Random vibration is typically studied in the frequency domain rather than the time domain (11) since the frequency content of the response can be easily understood from knowledge of the natural vibration modeshapes. One study of random vibration in the frequency domain is termed a Power Spectral Density (PSD) analysis. Using this study, a quantity in the frequency domain, such as PSD acceleration, is related to the square (or power) of physical acceleration in the time domain through Fourier transform techniques. The input PSD is a statistical description of the random vertical surface or profile in the frequency domain. Thompson (6) shows that a random function such as the road surface can be represented in the time domain by a Fourier series of the form

$$W(t) = (\text{Real part of}) \sum_n W_n(\omega_n)\, e^{j\omega_n t}$$

and

$$\overline{W^2(t)} = \sum_n \tfrac{1}{2}\left|W_n(\omega_n)\right|^2$$

where

W (t) is the time history of the road profile experienced by the road-tire interface.

$W_n(\omega_n)$ is the amplitude of the n-th harmonic representation of W (t).

$\overline{W}^2$ (t) is called the mean square value of the random road surface taken over a finite length of time.

The PSD input of the terrain $P_i(\omega)$ is defined such that

$$P_i(\omega_n)\,\Delta\omega_n = \tfrac{1}{2}\left|\,W_n(\omega_n)\right|^2$$

as shown in Fig. 5. The area defined by $P_i(\omega_n)\,\Delta\omega_n$ is the contribution to the mean square of the input $\overline{W}^2$ (t) by the nth harmonic Fourier representation of $\overline{W}^2$ (t). Therefore, $P_i(\omega)$ shows the frequency content of the mean square of the random vertical displacement of the road surface and the total area of the function $P_i(\omega)$ integrated over all frequencies is equal to the mean square value, $\overline{W}^2$ (t).

The PSD input, also called the auto-spectral density, of right and left profiles for two road surfaces used for the truck vibration study are shown in Figs. 6 and 7. The cross-spectral density, not shown, is complex with real and imaginary parts, and it accounts for the phase relationship statistics between inputs on the left and inputs on the right. Road 1, Fig. 6, shows a significant differential amplitude level from right to left side of the road and is most noticeable from 5 to 10 hz. Road 2, Fig. 7, shows comparable amplitudes right to left up to 20 hz. The spikes in Road 2 starting at 7 hz are the first and higher harmonics of tar strip inputs in the road at 3 meter intervals.

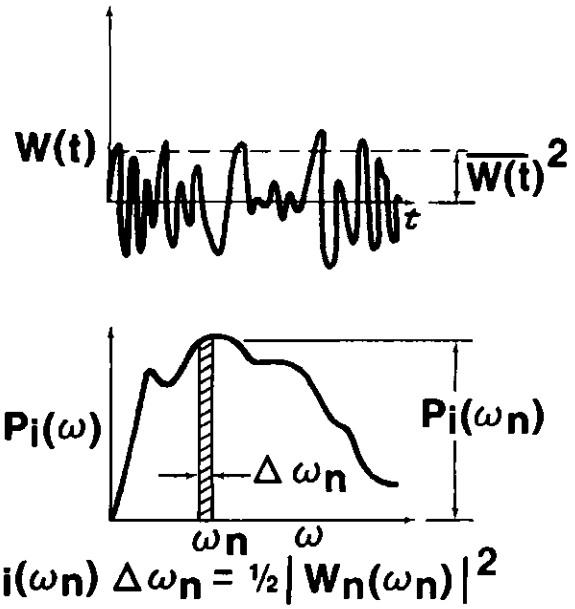

Fig. 5 - Power Spectral Density (PSD) definition

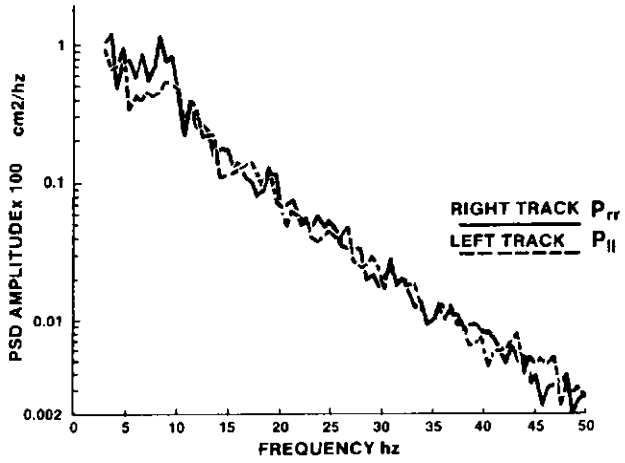

Fig. 6 - Random road input data for road surface No. 1

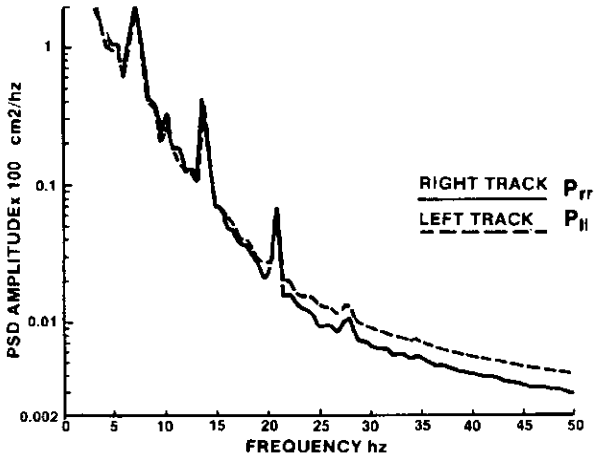

Fig. 7 - Random road input data for road surface No. 2

The PSD output response at a point in the vehicle, due to two random sources at the left and right tracks, is shown by Howell (12, 13) to be

$$P_o(\omega) = |H_l(\omega)|^2 P_{ll} + |H_r(\omega)|^2 P_{rr} + 2 \cdot (\text{Real part of}) [H_r(\omega) H_l(\omega)^* P_{lr}^*]$$

where

* implies complex conjugation

$H_l(\omega)$ is the transfer function due to left side unit loads at tire patch

$H_r(\omega)$ is the transfer function due to right side unit loads at the tire patch

P_{ll} is the left side input PSD

P_{rr} is the right side input PSD

P_{lr} is the cross-spectral density from left to right

The transfer function H (ω) includes the transmissibility of the tires and is non-dimensional (12). $P_o(\omega)$ defined above is the PSD displacement; however, the PSD acceleration is obtained by multiplying by ω^4 (14).

It can be seen that, the output PSD is a function of:

1. the square of the transfer function
2. the road input PSD function

Just as the frequency integral of the input PSD is the mean square of vertical road displacement, the integral of the output PSD acceleration is the mean square acceleration at the response point.

The following points should be made about the PSD analysis:

1. The phase relation between inputs from front to rear of the vehicle is accounted for in the transfer function (see Howell 12)

2. The phase relation between inputs from left to right is accounted for with the cross-spectral density (12).

3. No phase information between input and output is retained since only the magnitude of the transfer function is used to compute the output. However, it is generally assumed that the frequency content of the output amplitude is of prime importance (14).

MODESHAPE AND ROAD RESPONSE CORRELATION

Since the optimization program varies the mounting system of the vehicle model to arrive at improved ride characteristics, it is important that the model achieve a reasonable degree of correlation with the actual vehicle to assure that the results are meaningful. The natural vibration modeshapes and random road response obtained from analysis of the truck model were compared to test measurements of a prototype truck to establish the level of correlation.

TABLE 1
NATURAL VIBRATION FREQUENCY COMPARISON
PROTOTYPE TEST vs. MODEL ANALYSIS

Modeshape Description	Frequency (Hz) Test	Analysis
I. Rigid Body Motions		
Roll	1.4	1.5
Front bounce	1.5	1.6
Rear bounce	2.0	2.1
Pitch	2.7	3.4
II. Suspension Modes		
Front tramp	12.4	11.6
Front hop	12.0	11.9
Rear tramp	11.9	12.7
Rear hop	12.7	10.0
III. Structural Modes		
First torsion	7.4	8.2
First beaming	7.8	8.9
Cab yaw	10.0	11.7
Engine pitch	10.4	12.5
Engine pitch and cab bounce	13.1	14.3
Engine roll	13.9	13.3

MODESHAPE COMPARISON — The natural frequency of vibration of modeshapes of the prototype from testing are compared to the truck vehicle model in Table 1. The test measurements of the prototype are damped natural frequencies, whereas the frequencies from analysis of the model are undamped; however, the deviation is assumed negligible since damping is generally on the order of 3-6% of critical damping for structural modes (10).

The ride motion frequencies in Table 1 are all below 5 hz and the suspension modes are near 12 hz. These are typical values (15) for a vehicle of this design and can be used as a check on the basic modeling of the vehicle, especially when a prototype is not available for testing. The first beaming and torsional modes of the vehicle structure show good correlation between test and model and are dominated by the frame beaming and torsional component modeshapes.

Structural modes in Table 1 above 10 hz contained a fair amount of motion among several different components making it difficult to distinguish when modeshapes were identical. To overcome this, the dominant motion of the modeshape in both prototype and the model was used to decide if the mode was similar.

The distribution of kinetic and potential energy throughout the vehicle model for every modeshape was found using a NASTRAN post processor developed by GM Engineering Staff called ENERGY. The energy distribution must be closely studied in conjunction with the modeshape to properly understand the modeshape vibration characteristics (10).

RANDOM ROAD RESPONSE COMPARISON — The PSD acceleration frequency response at the left front floor attachment of the seat track, for two road surfaces, is compared between the model and the prototype test in Fig. 8 thru 11. Acceleration at the seat track was studied because it is related to the level of vibration experienced by the passenger (16). Acceleration levels in the lateral and vertical directions are reported here since it is believed that peak responses in these directions are the most significant to ride quality. The PSD amplitude is expressed in db's = 10 log (PSD acceleration) where the acceleration units are G^2/hz.

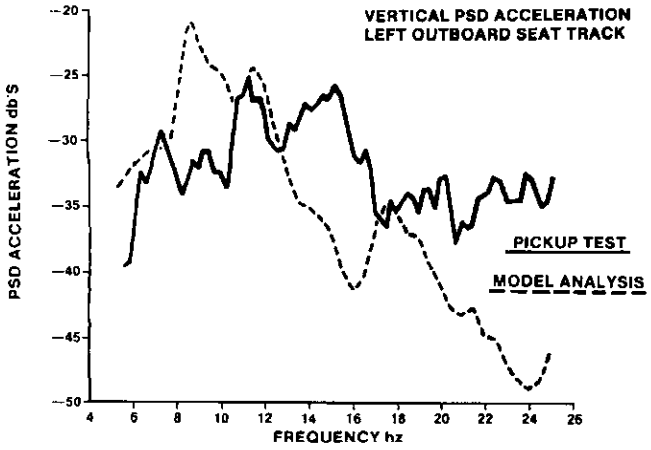

Fig. 8 - Vertical response on road No. 1 test compared to analysis

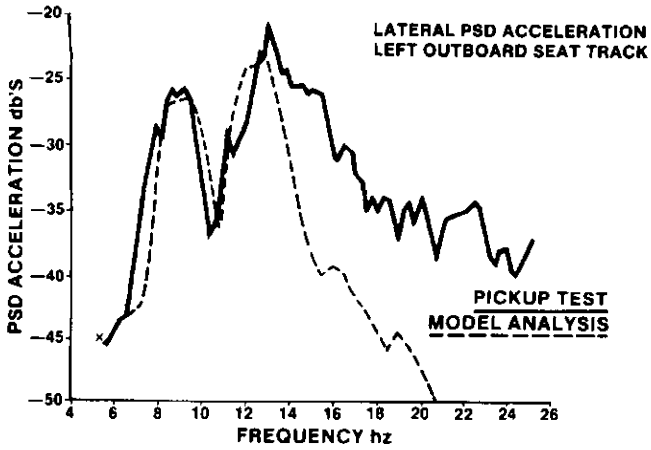

Fig. 9 - Lateral response on road No. 1 test compared to analysis

Modal participation factors (17) determine the amount of participation or contribution that each of the vehicle vibration modes makes to the amplitude of the response at a chosen frequency. These factors are found using a post-processor to NASTRAN called MPN, developed by GM Engineering Staff. The frequencies at the peak response amplitudes and the two participating vehicle normal modes which are the largest contributors to the peak accelerations, are shown in Tables 2 and 3, for both road surfaces.

TABLE 2
VEHICLE MODAL PARTICIPATION AT RESPONSE PEAKS
ROAD NO. 1 INPUT

Response peak	Largest contributor		Second largest contributor		
f (hz)	f (hz)	Description	f (hz)	Ratio*	Description
I. Vertical acceleration at seat track					
8.6	8.2	First torsion	8.9	.69	First beaming
11.4	8.2	First torsion	8.9	.46	First beaming
II. Lateral acceleration at seat track					
8.6	11.6	Front tramp	8.2	.76	First torsion
13.0	11.7	Cab yaw	12.7	.79	Rear tramp

TABLE 3
VEHICLE MODAL PARTICIPATION AT RESPONSE PEAKS
ROAD NO. 2 INPUT

Response peak	Largest contributor		Second largest contributor		
f (hz)	f (hz)	Description	f (hz)	Ratio	Description
I. Vertical acceleration at seat track					
7.2	1.6	Front bounce	8.9	.88	First beaming
9.0	8.9	First beaming	8.2	.59	First torsion
11.6	8.2	First torsion	1.6	.74	Front bounce
II. Lateral acceleration at seat track					
9.0	11.6	Front tramp	11.7	.60	Cab yaw
12.6	11.7	Cab yaw	12.7	.77	Rear tramp

* Ratio is the fraction of contribution relative to the largest contributor.

Comparing the vertical accelerations in Fig. 8 for road 1, the first peak occurs near 8 hz for both prototype and model, but they deviate in amplitude. Modal participation in Table 2 shows the peak for the model is at 8.6 hz and results primarily from first torsion. This appears reasonable since first torsion for the model and the prototype are near this frequency. The peak near 11. hz shows good correlation in amplitude and frequency. Although modal participation at 11.4 hz is still dominated by torsion and beaming, a close examination of participating modes smaller than the two largest shows that the suspension modes contribute more to this peak, as would be expected from the natural frequencies for both model and prototype. Comparing the lateral accelerations in Fig. 9 for road 1, shows that very good correlation with response peaks has been achieved at 9 and 13 hz. Both lateral and vertical acceleration for the model deviate below the prototype level above 14 hz.

The vertical accelerations in Fig. 10 for road 2 show good correlation between model and prototype for peaks near 8 and 11 hz. The lateral accelerations in Fig. 11 show the same general trend up to 14 hz, but deviate slightly in amplitude and frequency.

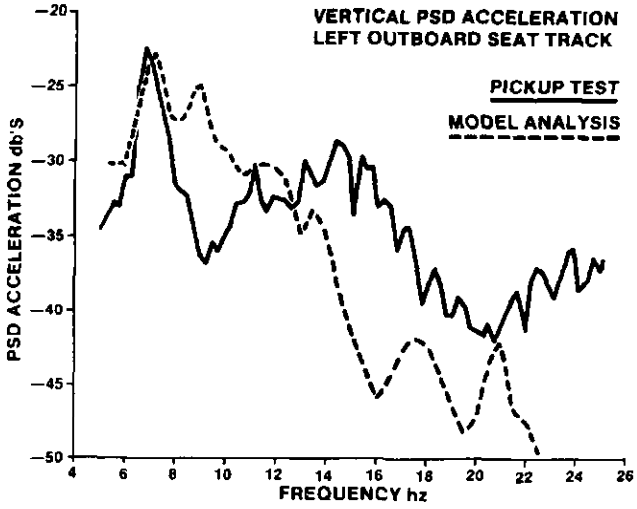

Fig. 10 - Vertical response on road No. 2 test compared to analysis

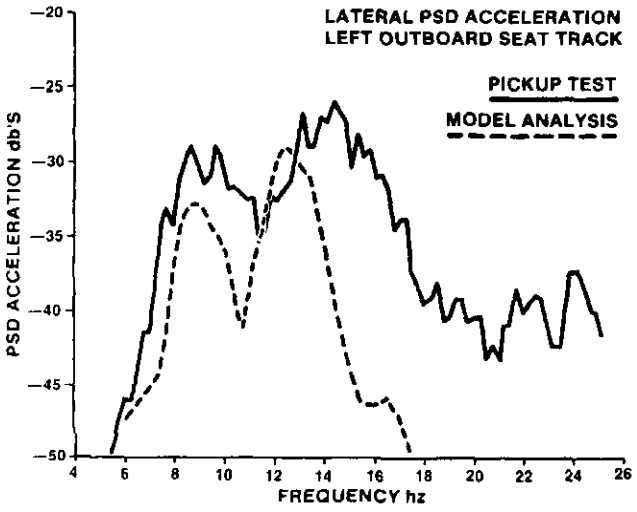

Fig. 11 - Lateral response on road No. 2 test compared to analysis

An examination of the response curves shows that the analytical response deviates below test response at frequencies greater than 14 hz. Due to the many approximations that have been made and the complexity of the problem, it is difficult to determine the exact source of deviation. Part of the deviation is attributed to the loss in accuracy observed for structural modes higher than 14 hz. Nonlinear effects are additional sources of deviation which include shock absorber characteristics, body mount and suspension bushing characteristics (10), loss of contact between tire and road surface, friction effects such as in leaf springs, etc.

In general, the random road results of the model show acceptable correlation with that of the prototype in the areas of peak response accelerations. The data for the tested PSD response was performed only once for one vehicle, and thus there was no data available on the variability of test results. For a given road and vehicle some of the sources of variability of test results (18) are: (1.) Operating speeds, (2.) Atmospheric conditions (temperature - see ref. 6), (3.) The path followed by the vehicle along the surface, and (4.) Errors in instrumentation.

An examination of the road input PSD and modal participations for both road surfaces results in the following observations: (1.) The difference in input amplitude from right to left for road 1 from 5 to 10 hz results in vertical accelerations which are dominated by anti-symmetric modes, (2.) The in phase amplitude nature of road 2 and the spike at 7 hz results in vertical accelerations, which are dominated by symmetric modes. Thus, it should be reiterated that the PSD response is a function of the road as well as the inherent vibration properties of the structure.

OPTIMIZATION PROCEDURE

During the development of the ride quality of a vehicle, the ride development engineer will ride the vehicle over various terrains to subjectively evaluate the response to random road roughness and the sensitivity of the vehicle to tire unbalance and nonuniformities. Then, based on experience and the subjective evaluation, he will begin a phase of development called "mount tuning" where an array of rubber isolator mounts with various stiffness rates will be road tested until a satisfactory ride is achieved. As can be imagined, the process is time consuming and relies largely on a trial and error process.

The goal of the mount optimization procedure is to arrive at an initial mount system that will more closely estimate the best mount configuration. The available development time could be used to arrive at overall improved ride quality compared to that achievable by trial and error alone. If the results of mount optimization for the vehicle model do not reduce vehicle vibration to acceptable levels, then the basic vehicle structure can be examined for cost effective and mass efficient modifications to further reduce the vibration. The analysis discussed here varies the mount system only.

A program developed by GM Engineering Staff called NASTUNE was used to perform the mount optimization. NASTUNE uses an optimization program called CONMIN described in ref. (19).

The CONMIN technique has been used by Bennett to optimize the structural properties of a body structure (19), by Baum to study semi-tractor ride improvement (20), and by Johnson to optimize an engine mounting system (21). The essence of the optimization procedure (21) is to minimize

$$F(x) = \sum_{i=1}^{n} WE_i [f_i(x) - g_{opt,i}]^2$$

subject to constraints $h_i(x) \leq o$

where

x is a vector of design variables

$\bar{F}(x)$ is the objective function to be minimized

$f_i(x)$ is the value of the i-th performance variable

$g_{opt,i}$ is the desired value of the i-th performance variable

WE_i is a user chosen weighting factor

n is the number of performance variables

The mount system tuning variables for the truck vibration optimization consisted of body, engine, and transmission rubber mounts shown schematically in Fig. 12. Six body mounts isolate the cab-FESM combination from the frame. The engine and transmission vibrations are isolated from the frame with three mounts.

The load cases considered for the response included random road 1 and all 12 tire force inputs which were optimized simultaneously. Road 1 was chosen for optimization since prototype ride evaluations indicated an unsatisfactory ride on this road.

The stiffness rates of the mounts, the design variables, were allowed to vary within upper and lower bound constraints. The quantities to be reduced, the performance variables, were the acceleration levels at the seat track and toe panel of right and left sides. These performance variables were the acceleration amplitudes for a range of discrete frequencies centered around peaks in the response and were summed over all of the dynamic load cases to form the objective function, the quantity to be minimized. The desired value of each performance variable was chosen as o., and all weighting factors were unity.

The maximum response amplitudes contribute the most to the magnitude of the objective function; therefore, the major effect of the solution obtained by the optimizer will be to reduce the maximum or peak values of the response. For the random road load case, the response amplitudes in the frequency range from 6 to 14 hz at intervals of .33 hz were used to form the objective function. Each tire force load case was optimized at 11.0, 13.25, and 15.75 hz.

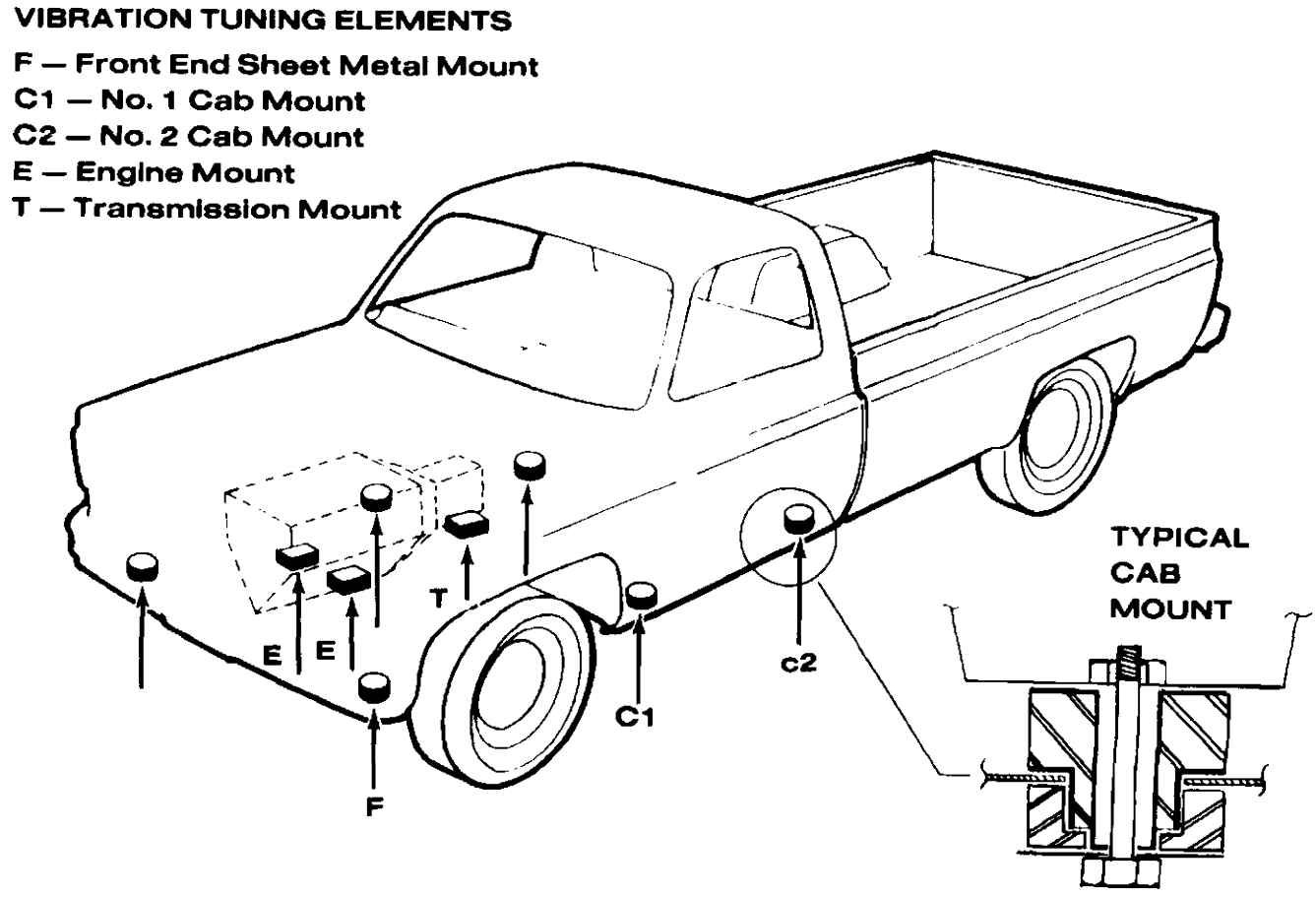

Fig. 12 - Location of rubber vibration isolators for mount system optimization

A perturbation technique is a key element of the optimizer, since it must evaluate the vehicle response for many mount rate changes. A technique described by Vail (22) shows that a new free vibration equation of motion can be formulated from changes in mount rate stiffness as follows:

$$\{-\omega^2 [M] + [K] + \phi^T \Delta k \phi]\} \{s\} = 0$$

where

Δk is the change in mount stiffness between attaching components.

ϕ is the original vehicle modeshape matrix.

M and K are the original vehicle modal mass and stiffness. Note that his equation has a form similar to Eq. 8 which was derived for the actual spring rate between attaching components. Damping terms and the original force vectors are added to the equation to find the forced response solution.

Note that the perturbation solution is an approximation which uses the base vehicle modeshapes but accounts for small stiffness changes in the system. Experience has shown that it is accurate when compared to the exact analysis which accounts for stiffness changes in the K matrix of eq. 10 before the modeshapes are calculated. The perturbation solution is simplified since it does not require an eigenvalue solution and it uses the reduced set of original vehicle modeshapes.

The process flow schematic for the optimization program is shown in Fig. 13. The first step is the input of control data which describes the type of analysis, design variable bounds, the performance variables to be minimized, and weighting factors. Secondly, the original system modeshape properties and force vectors are read into the optimizer. Thirdly, the search technique varies the design variables within their bounds, makes calls to and receives the results of changes from the perturbation analysis, and continues the process until a minimum is found or the constraints limit further iteration. Lastly, the optimized system of mounts is checked using the exact analysis to verify the approximation made with the perturbation analysis.

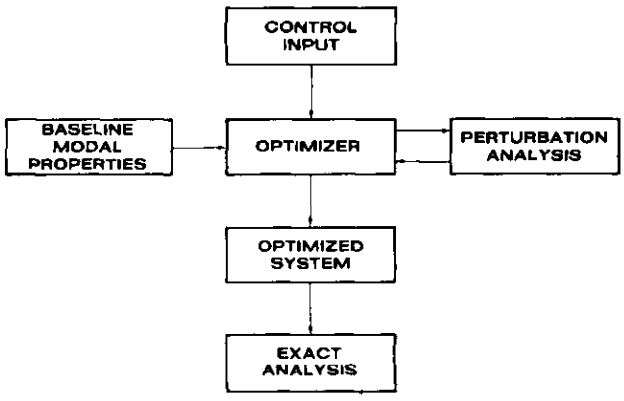

Fig. 13 - Optimization program flow chart

TABLE 4
ORIGINAL AND OPTIMIZED MOUNT RATES
(N/cm)

	ORIGINAL	OPTIMIZED	CHANGE
FESM mount			
vertical	5510	5270	- 4.4%
lateral	1700	1290	- 24.%
fore-aft	3500	1300	- 63.%
Cab 1 mount			
vertical	10940	21000	+ 93.%
lateral	6700	16600	+150.%
fore-aft	4200	5360	+ 28.%
Cab 2 mount			
vertical	7240	5210	- 28.%
lateral	2940	1310	- 55.%
fore-aft	2940	1410	- 52.%
Engine mount			
vertical	14000	17600	+ 26.%
lateral	4400	5180	+ 18.%
fore-aft	3000	3610	+ 20.%
Trans. mount			
vertical	4760	5050	+ 6.1%
lateral	2850	2840	0.
fore-aft	6220	6390	+ 2.7%

MOUNT SYSTEM OPTIMIZATION RESULTS

The set of original mount rates is shown in Table 4 along with the set of rates obtained from the optimization. The most significant changes occured at the cab No. 1 mount vertical rate and the lateral and fore-aft rates of the FESM, cab No. 1, and cab No. 2 mounts.

Constraints were placed on the ratios of the lateral and fore-aft body mount rates to that of the vertical rate to assure that the optimized body mount was a feasible design. The vertical rate was allowed to vary within bounds while lateral and fore-aft rates were constrained

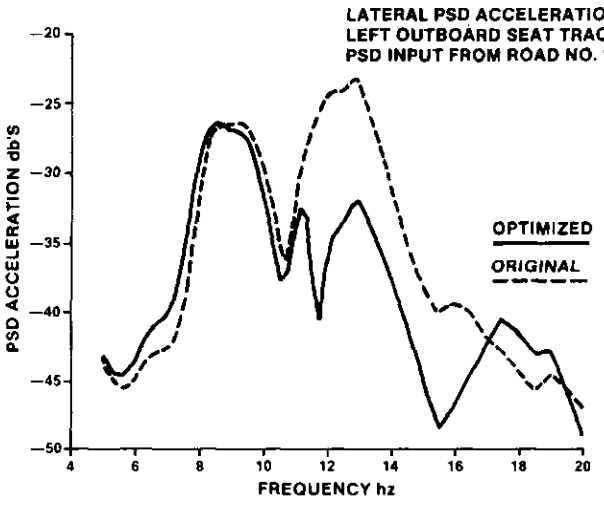

Fig. 14 - Lateral response of optimized compared to original mount system

to range from .25 to .80 that of the vertical rate. In addition, the body mounts on the right side of the vehicle were constrained to have the same rates as those on the left. The engine and transmission mount rates were constrained similarly except that the ratio of lateral and fore-aft rates to the vertical rate was tightly constrained so that the original and optimized ratios would be equal.

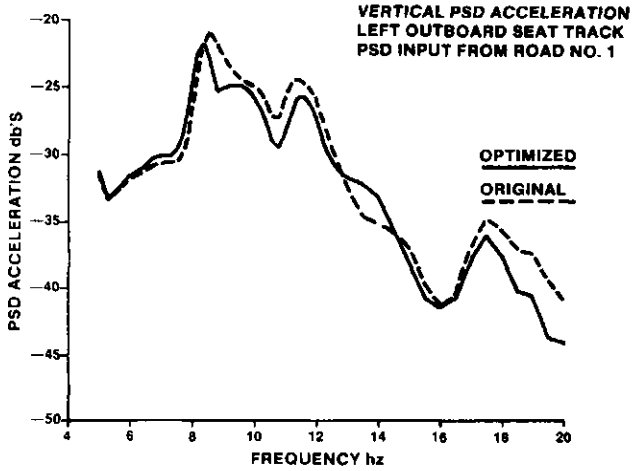

Fig. 15 - Vertical response of optimized compared to original mount system

Response plots of the PSD acceleration on road 1 in Figs. 14 and 15 compare the optimized mount system to the original mounts. The most significant change was a reduction in lateral response from 11 to 17 hz shown in Fig. 14. The vibration modes of the optimum mount system show that the cab yaw mode, shown in Fig. 16, originally at 11.7 hz has been reduced to 9.8 hz as would be expected intuitively due to the reduction in fore-aft and lateral rates at FESM and cab No. 2 mounts. The yaw mode consists of a rigid body yaw motion of the cab with most of the strain energy concentrated in the mounts. At the new frequency, the cab yaw mode has been separated in frequency from the rear suspension tramp mode, thus resulting in a reduction in lateral response.

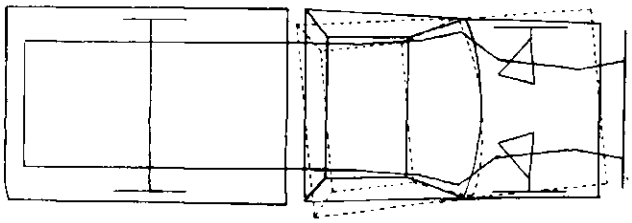

Fig. 16 - Cab yaw vibration modeshape

The change in vertical response is more subtle than the lateral; however, the dominant effect is due to a change in engine pitch mode which causes it to couple with the front suspension modes and act as a dynamic absorber (23) to reduce response from suspension resonance. The relatively small changes in vertical response are due to the fact that the dominant vehicle modes, beaming and torsion, are dominated by the frame beaming and torsion modes and are virtually insensitive to the mount rates.

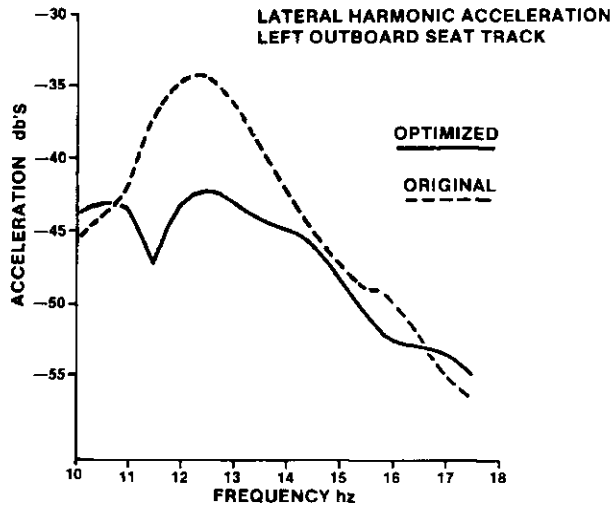

Fig. 17 - Lateral harmonic response to rear tire radial force variation

The lateral and vertical acceleration response due to harmonic tire radial force variation on the left side of the vehicle is compared for original and optimum mounts in Figs. 17 and 18. The harmonic response is expressed in db's = 20 log (G's). All tire harmonic inputs were optimized at three discrete driving speeds, 72, 88, and 104 Km/hr, which correspond to 11.0, 13.25, and 15.75 hz for the first harmonic of tire force. Tables 5 and 6 compare the mean accelerations between the original and optimized mount systems for response at the left seat track and at the approximate location where the driver would place his feet, called the left toe panel. The frequency range for the mean acceleration calculation was from 11 to 16 hz which includes the optimization frequencies. The response levels due to tire-wheel unbalance loads were small relative to the tire force variation responses and are not shown in Tables 5 and 6.

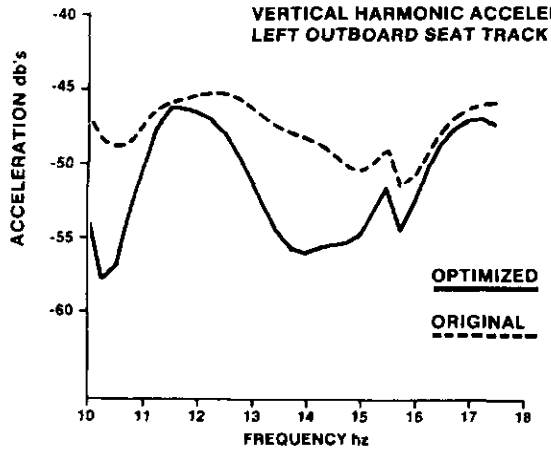

Fig. 18 - Vertical harmonic response to rear tire radial force variation

TABLE 5
LEFT SEAT TRACK HARMONIC RESPONSE AMPLITUDE (G's x 1000)
Mean acceleration level from 11 to 16 hz

Left tire force variation	Lateral acceleration			Vertical acceleration		
	Original	Optimized	Change*	Original	Optimized	Change
Front radial force	4.3	3.2	-10.%	8.0	6.4	-14.%
Rear radial force	11.2	5.8	-47.%	4.5	3.0	-13.%
Front lateral force	11.1	9.7	-12.%	9.0	7.9	-10.%
Rear lateral force	11.1	7.2	-34.%	3.8	3.4	-3.0%

TABLE 6
LEFT TOE PANEL HARMONIC RESPONSE AMPLITUDE (G's x 1000)
Mean acceleration level from 11 to 16 hz

Left tire force variation	Lateral acceleration			Vertical acceleration		
	Original	Optimized	Change	Original	Optimized	Change
Front radial force	3.3	3.5	+2.2%	6.5	5.8	-6.1%
Rear radial force	3.7	6.0	+20.%	2.3	1.6	-6.1%
Front lateral force	11.5	7.7	-33.%	4.9	4.2	-6.1%
Rear lateral force	3.9	8.0	+36.%	1.9	1.5	-3.5%

* *The base for change calculations is the maximum original mean acceleration* = 11.5 at toe panel due to front lateral force.

Reductions in acceleration levels in the seat track lateral and vertical responses are shown in Table 5. The percent change calculation is relative to a common base of .0115 G's which is the maximum mean acceleration for all cases and occurs at the toe panel due to front lateral tire force variation. A common base is necessary to properly evaluate the significance of changes among all of the mean values.

It can be seen from Table 6 that the toe panel lateral accelerations have increased for three load cases. This results from the compromise that takes place as the optimizer seeks out the overall minimum response solution. Three points should be emphasized from the data:

1. Toe panel lateral response has increased for three cases, but it has been reduced for the remaining case which initially had the significantly larger mean value.
2. Each of the responses that increased for the toe panel accelerations were initially lower than the corresponding accelerations at the seat track which have decreased.
3. The final optimized mean lateral acceleration levels at the seat track and toe panel for the same load case, have approximately the same mean value.

Therefore, the optimization process has resulted in mean acceleration levels that have been evened out throughout the vehicle as would be desired. If more improvement at the seat track were desired at the expense of the toe panel, it could be done by weighting the seat track response higher with WE_i.

The final merit of any design optimization must address the question of how much improvement it will provide for the customer. To answer this question it would be desirable to relate the quantitative improvements in the seat track PSD accelerations to the subjective rating of the passenger. This relation would provide the ability to quantitatively predict the improvement in ride quality due to design modifications before a future vehicle is built and ridden.

This area is still a subject for debate; however, Smith, McGehee, and Healy (16) have shown that a high degree of correlation can be obtained between RMS (root mean square) acceleration at the floor panel and the personal subjective evaluation of the passenger. Their work correlated the personal ratings of various passengers using a subjective scale of five points (five being the best ride) to the RMS acceleration of two separate vehicles over various road surfaces. Their relationship, after conversion to a ten point rating scale, is MPR = 10.9 - 80.0A, where MPR is the "mean personal rating," based on ten being the best ride, and A is the "magnitude" of combined RMS lateral and vertical acceleration from 0 to 40 hz. The RMS acceleration is the square root of the mean square response, defined in section 2 as the frequency integral of the PSD response P_o.

$$\text{RMS} = \sqrt{\int_0^{40\ \text{hz}} P_o(f)\, df}$$

and

$$A = \sqrt{(\text{RMS LATERAL})^2 + (\text{RMS VERTICAL})^2}$$

Based on this rating relation, a change of -.0125 G's in A corresponds to one rating point of improvement.

The RMS accelerations at the seat track for road 1 were calculated from 0 to 40 hz for the vehicle model in lateral and vertical directions. The change in magnitude, A, of RMS acceleration for the optimized system relative to the original system was -.0330 G's. Thus, by this criterion, the personal subjective improvement in ride quality would be 2 and 1/2 rating points.

SUMMARY

The basic relations applicable to vehicle modeling have been reviewed including the concepts of modal truncation, local compliance, component coupling, and vehicle modal synthesis. Each component modal representation was shown to consist of a set of natural vibration properties including modal mass, modal stiffness, and modeshape. The components were coupled together using local compliance and rubber mount springs and assembled to the suspension and driveline to synthesize a complete pickup truck vehicle model.

The model vibration response was analyzed due to dynamic loads induced by tire and wheel nonuniformity and from random road surfaces. The vibration response of the model on two random road surfaces compared to measurements of a prototype vehicle show acceptable correlation with the peak amplitude and frequency of response.

The mount tuning phase of vehicle ride development is an extremely time consuming process requiring significant ride experience and many ride iterations by the engineer. An optimization technique was applied to the model to find the best engine, transmission, and body mount system from a continuous range of mount rates, subject to specified bounds, to arrive at improved vehicle ride quality. The results for the optimized mount system show reductions in mean acceleration for the model of up to 47% for tire induced vibration. The random road response improvement in subjective ride quality predicted by the model based on a modified 10 point scale proposed by Smith et al. (16) was found to be 2 and 1/2 rating points.

Modal modeling techniques provide an improved understanding of vehicle vibration characteristics. The use of an optimization technique to compliment the vehicle ride development process indicates significant savings in time and the potential for approaching optimum ride quality.

ACKNOWLEDGEMENT

The author would like to thank James Partyka who helped with modeling and analysis of the vehicle. Thanks also goes to Ashok Aguiar, Paul Tsai, and fellow colleagues for their helpful suggestions and encouragement. The General Motors Engineering and Research Staffs are greatly appreciated for assisting the application of the engineering tools they have developed and for sharing their design experience.

REFERENCES

1. W. A. Benfield and R. F. Hruda, "Vibration Analysis of Structures by Component Mode Substitution," AIAA Journal, Volume 9, No. 7, July 1971, pp. 1255-1261

2. A. A. Butkunas, "Power Spectral Density and Ride Evaluation," SAE Paper No. 660138, 1966

3. G. E. Townley and Joseph W. Klahs, "Dynamic Simulation of an Automobile Body Utilizing Finite Element and Modal Synthesis Techniques," SAE Paper No. 780364, February 1978

4. L. Meirovitch, "Analytical Methods in Vibrations," The Macmillan Company, 1967.

5. S. C. Walgrave and James M. Ehlbeck, "Understanding Modal Analysis," SAE Paper No. 780695, August 1978

6. W. T. Thompson, "Vibration Theory and Applications," Prentice-Hall Inc., 1965

7. R. J. Guyan, "Reduction of Stiffness and Mass Matrices," AIAA Journal, Vol. 3, No. 2, Feb. 1965, p. 380

8. M. F. Nelson, "The Use of Condensation Techniques for Solving Dynamics Problems," SAE Paper No. 740330, March 1974

9. W. A. McClelland and A. L. Klosterman, "NASTRAN for Dynamic Analysis of Vehicle Systems," SAE Paper No. 740326, March 1974

10. J. C. Davis, "Modal Modeling Techniques for Vehicle Shake Analysis," SAE Paper No. 720045, January 1972

11. W. F. Lins, "Vehicle Vibration Analysis Using Frequency Domain Techniques," Journal of Engineering for Industry, Trans. ASME, Vol. 91, Nov. 1969, p 1075 -1080

12. L. J. Howell, "Power Spectral Density Analysis of Vehicle Vibration Using the NASTRAN Computer Program," SAE Paper No. 740328, March 1974

13. L. J. Howell, Private communication, March 29, 1981

14. B. D. Van Duesen, "Analytical Techniques for Designing Riding Quality into Automotive Vehicles," SAE Transactions, Vol. 76, Paper No. 670021, 1967

15. J. S. Majcher, et. al., "Analysis of Vehicle Suspensions with Static and Dynamic Computer Simulations," SAE Paper No. 760183, February 1976

16. C. C. Smith, et. al., "The Prediction of Passenger Riding Comfort from Acceleration Data," Transactions of the ASME, Vol. 100, pp 34 - 41, March 1978

17. M. M. Kamal and J. A. Wolf, "Finite Element Models for Automotive Vehicle Vibrations," 1977 ASME Vibrations Conference, September 26 - 26, 1977

18. A. A. Butkunnas, "Random Vibration Analysis and Vehicle Development," SAE Paper No. 690109, 1969

19. J. A. Bennett and M. F. Nelson, "An Optimization Capability for Automotive Structures," SAE Paper No. 790972, October 1979

20. J. H. Baum, et. al., "Truck Ride Improvement Using Analytical and Optimization Methods," SAE Paper No. 770609, April 1977

21. S. R. Johnson and J. W. Subhedar, "Computer Optimization of Engine Mounting Systems," SAE Paper No. 790974, October 1979

22. C. F. Vail, "A Modal Synthesis Technique for Determining Dynamic Properties of a Structure for Mass and Stiffness Changes," SAE Paper No. 740329, March 1974

23. F. Everett Reed, "Dynamic Vibration Absorbers and Auxiliary Mass Dampers," Chap. 6, "Shock and Vibration Handbook," McGraw - Hill Book Co., New York, 1976